Acta Crystallographica Section D
Biological Crystallography
ISSN 0907-4449

Structure of the zinc-saturated C-terminal lobe of bovine lactoferrin at 2.0 Å resolution

Talat Jabeen, Sujata Sharma, Nagendra Singh, Asha Bhushan and Tej P. Singh*

Department of Biophysics, All India Institute of Medical Sciences, New Delhi 110 029, India

Correspondence e-mail: tps@aiims.aiims.ac.in

Received 21 February 2005
Accepted 19 May 2005

PDB Reference: zinc-saturated C-terminal lobe of bovine lactoferrin, 1sdx.

The crystal structure of the zinc-saturated C-terminal lobe of bovine lactoferrin has been determined at 2.0 Å resolution using crystals stabilized at pH 3.8. This is the first metal-saturated structure of any functional lactoferrin at such a low pH. Purified samples of proteolytically generated zinc-saturated C-terminal lobe were crystallized from 0.1 *M* MES buffer pH 6.5 containing 25%(*v*/*v*) polyethyleneglycol monomethyl ether 550 and 0.1 *M* zinc sulfate heptahydrate. The crystals were transferred to 25 m*M* ammonium acetate buffer containing 25%(*v*/*v*) polyethyleneglycol monomethyl ether 550 and the pH was gradually changed from 6.5 to 3.8. The X-ray intensity data were collected with a 345 mm imaging-plate scanner mounted on an RU-300 rotating-anode X-ray generator using crystals soaked in the buffer at pH 3.8. The structure was determined with the molecular-replacement method using the coordinates of the monoferric C-terminal lobe of bovine lactoferrin as a search model and was refined to an *R* factor of 0.192 for all data to 2.0 Å resolution. The final model comprises 2593 protein atoms (residues 342–676 and 681–685), 138 carbohydrate atoms (from 11 monosaccharide units in three glycan chains), three Zn^{2+} ions, one CO_3^{2-} ion, one SO_4^{2-} ions and 227 water molecules. The overall folding of the present structure is essentially similar to that of the monoferric C-terminal lobe of bovine lactoferrin, although it contains Zn^{2+} in place of Fe^{3+} in the metal-binding cleft as well as two additional Zn^{2+} ions on the surface of the C-terminal lobe. The Zn^{2+} ion in the cleft remains bound to the lobe with octahedral coordination. The bidentate carbonate ion is stabilized by a network of hydrogen bonds to Ala465, Gly466, Thr459 and Arg463. The other two zinc ions also form sixfold coordinations involving symmetry-related protein and water molecules. The number of monosaccharide residues from the three glycan chains of the C-terminal lobe was 11, which is the largest number observed to date. The structure shows that the C-terminal lobe of lactoferrin is capable of sequestering a Zn^{2+} ion at a pH of 3.8. This implies that the zinc ions can be sequestered over a wide pH range. The glycan chain attached to Asn545 may also have some influence on iron release from the C-terminal lobe.

1. Introduction

Lactoferrin is an 80 kDa bilobal glycoprotein. The two lobes are homologous and each contains a binding site for a metal ion. The antibacterial activity of lactoferrin is considered to be associated with its capacity to sequester ferric ions. The structural features of iron-bound lactoferrin from a number of species have been studied (Anderson *et al.*, 1989; Haridas *et al.*, 1995; Moore *et al.*, 1997; Sharma, Parmasivam *et al.*, 1999; Sharma, Kumar *et al.*, 1999; Karthikeyan *et al.*, 1999, 2002).

The structures of apolactoferrins have also been determined from several sources (Anderson *et al.*, 1990; Jameson *et al.*, 1998; Sharma, Rajashankar *et al.*, 1999; Khan *et al.*, 2001; Kumar *et al.*, 2002). The presence of two homologous N- and C-terminal lobes in lactoferrin gives rise to a number of questions concerning the purpose of their coexistence as well as the sustainability of their functional viability on decoupling, the precise role of interlobe interactions, the functional interdependence of the N- and C-terminal lobes, the structural features of monoferric lobes and the roles of other metal ions which can replace the ferric ion and the features of their apo forms. It may be mentioned here that the attempts have been made in the past to generate the N- and C-terminal lobes proteolytically (Brock & Arzabe, 1976; Brines & Brock, 1983). However, owing to the fortuitous nature of enzymatic digestion, this method did not yield the required molecular halves of lactoferrin. Therefore, further efforts were directed to prepare N- and C-terminal lobes using cloning methods. As a result, the N-terminal lobe and several mutants were cloned and their structures were analyzed successfully (Day *et al.*, 1992; Faber, Baker *et al.*, 1996; Faber, Bland *et al.*, 1996; Nicholson *et al.*, 1997; Peterson *et al.*, 2000, 2002; Jameson *et al.*, 2002). The C-terminal lobe was reported to be expressed poorly, probably owing to the absence of an efficient C-terminal lobe recombinant expression system (unpublished results). Hence, the isolated C-terminal lobe has not been studied crystallographically. However, parallel efforts continued to prepare the N- and C-terminal lobes proteolytically. The attempts were successful in the case of transferrins and the crystal structures of several fragments of ovotransferrin including N- and C-terminal lobes have been determined (Lindley *et al.*, 1993; Dewan *et al.*, 1993; Mizutani *et al.*, 1999; Mizutani, Mikami *et al.*, 2001; Mizutani, Muralidhara *et al.*, 2001). In this context, the most important difference between the structures of transferrins and lactoferrins is the conformation of the interlobe peptide, which has an extended structure in transferrins and a helical conformation in lactoferrins. This might account for the lack of success in hydrolyzing ovotransferrin or lactoferrins with enzymes such as trypsin, chymotrypsin and pepsin (Brock & Arzabe, 1976; Brines & Brock, 1983). Eventually, the two desired molecular halves (the N- and C-terminal lobes) of lactoferrin were produced proteolytically using the enzyme proteinase K (Singh *et al.*, 1998; Sharma, Singh *et al.*, 1999). The first crystal structure of the proteolytically generated monoferric C-terminal lobe of bovine lactoferrin has recently been determined (Sharma *et al.*, 2003). The structure revealed the presence of two zinc ions on the surface of the C-terminal lobe, indicating a feature apparently unique to the isolated C-terminal lobe. In order to assess the significance of zinc ions with respect to lactoferrin, the binding properties of zinc ions with C-terminal lobes of various lactoferrins were also studied (unpublished data). In the present paper, we report the crystal structure of a zinc-saturated C-terminal lobe that has been produced proteolytically from diferric lactoferrin. The crystals of the zinc-saturated C-terminal lobe were incubated in a solution of 25%(*v*/*v*) polyethyleneglycol monomethyl ether 550 and 25 m*M* ammonium acetate buffer pH 3.8 for one week. The structure revealed the presence of an octahedrally coordinated Zn^{2+} ion at the metal-binding cleft of the C-terminal lobe. Two additional zinc ions were also located at the surface of the molecule, which also formed similar octahedral coordinations with symmetry-related molecules in the crystals. These studies have also shown that the zinc remained bound to the C-terminal lobe to a much lower pH than reported for the ferric ion and thus suggest that lactoferrin can retain bound Zn^{2+} ions at a much lower pH than for Fe^{3+} ions.

2. Materials and methods

2.1. Preparation of N- and C-terminal lobes

Lyophilized samples of bovine lactoferrin were obtained from Morinaga Co., Japan. These were saturated with ferric ions and hydrolyzed with proteinase K as reported previously (Sharma *et al.*, 1999). The N- and C-terminal lobes were separated from the digests on a column (150 × 15 mm) of CM-Sephadex C-50 using a salt gradient of 0.0–0.5 *M* NaCl in 50 m*M* Tris–HCl pH 8.0. The separated peaks of the N- and C-terminal lobes were further purified independently on a gel-filtration column (100 × 15 mm) of Sephadex G-75 in 50 m*M* Tris–HCl pH 8.0.

2.2. Preparation of the Zn^{2+}-saturated C-terminal lobe

In order to prepare the Zn^{2+}-saturated C-terminal lobe, it was first converted into an apo form. The procedure developed by Masson & Heremans (1968) was followed. The purified C-terminal lobe solution (1% in distilled water) was dialyzed against an excess of 0.1 *M* citric acid with regular changes after every 6 h. Citric acid was removed by dialysis against an excess of distilled water with regular changes after every 6 h for 24 h at 277 K. The colourless apoprotein was lyophilized. It was dissolved in 0.1 *M* sodium bicarbonate/sodium citrate buffer, 2 m*M* $ZnSO_4$ at pH 8.6 and equilibrated for 16 h at room temperature. The zinc-saturated C-terminal lobe was used for crystallization.

2.3. Dynamic light scattering

Dynamic light-scattering (DLS) measurements were made on the samples of bovine lactoferrin, the monoferric C-terminal lobe and the zinc-saturated C-terminal lobe. The studies were carried out with a DLS system (RiNA, Berlin, Germany) and the results were analyzed using the software described by Schulze (1996). The sample solutions were prepared in the following buffers: intact diferric lactoferrin was dissolved in 25 m*M* Tris–HCl pH 8.0, 8%(*v*/*v*) 2-methyl-2,4-pentanediol (MPD) and 10%(*v*/*v*) ethanol, the monoferric C-terminal lobe was dissolved in 0.1 *M* MES pH 6.5 containing 25%(*v*/*v*) polyethylene glycol monomethyl ether 550 and 0.01 *M* zinc sulfate heptahydrate and the zinc-saturated C-terminal lobe was dissolved in 25 m*M* ammonium acetate buffer pH 3.8 containing 25%(*v*/*v*) polyethylene glycol monomethyl ether 550 and 0.01 *M* zinc sulfate. The concentrations of all the samples were maintained at 5 mg ml^{-1}.

Table 1
Data-collection statistics.

Values in parentheses are for the highest resolution shell (2.1–2.0 Å).

Space group	$P2_1$
Unit-cell parameters (Å)	
a	63.2
b	50.5
c	66.1
Z	2
V_M (Å^3 Da^{-1})	2.5
Solvent content	51
Resolution range (Å)	20.0–2.0
Total No. of measured reflections	140559
No. of unique reflections	24896
Completeness of data (%)	91.0 (75.0)
R_{sym} (%)	7.9 (31.5)
$I/\sigma(I)$	14.7 (2.2)

Table 2
Refinement statistics.

PDB code	1sdx
Resolution limits (Å)	20.0–2.0
No. of reflections	24896
R_{cryst} (%)	19.2
R_{free} (%)	21.0
Protein atoms	2593
Zinc ions	3
Carbonate ions	1
Sulfate ions	1
Sugar residues	11 (138 non-H atoms)
Water molecules	227
R.m.s.d in bond lengths (Å)	0.009
R.m.s.d in bond angles (°)	2.1
R.m.s.d in torsion angles (°)	23.9
Overall *G* factor	0.10
Mean *B* factor for main-chain atoms	33.8
Mean *B* factor for side-chain atoms and waters	44.0
Mean *B* factor for all atoms	39.8
Residues in most allowed regions (%)	88.7
Residues in additionally allowed regions (%)	9.3
Residues in generously allowed regions (%)	1.7
Residues in disallowed regions (%)	0.3

After filtration through 0.1 µm polyvinylidene difluoride filters (Millipore, Bedford, USA), the samples were manually injected into the flow cell (50 µl) and illuminated with a 25 mW, 600 nm solid-state laser. The data were measured three times and averaged.

2.4. Analysis of zinc and iron release

The zinc and iron were removed in a stepwise manner. The purified zinc- and iron-saturated samples of the C-terminal lobe were prepared at 1% concentrations in 50 m*M* Tris–HCl pH 8.0 and were dialyzed against an excess of 0.1 *M* citric acid with regular changes of dialysis buffer, with a fresh buffer change after every 6 h. At every step, the pH was adjusted with NaOH to the required value. The pH range was varied from pH 8.0 to 2.0 in pH intervals of 0.5. The dialysis experiments were carried out at each pH value for 24 h. At every pH value, the zinc and iron saturation were estimated from the ratios A_{526}/A_{280} and A_{465}/A_{280}, respectively. These ratios were used to estimate the degree of zinc and iron saturation of the C-terminal lobe.

2.5. Crystallization of zinc-saturated C-terminal lobe

A 50 mg ml^{-1} protein solution in deionized water was mixed in a 1:1 ratio with the crystallization buffer [0.1 *M* MES pH 6.5, 25%(*v*/*v*) polyethylene glycol monomethyl ether 550 and 0.01 *M* zinc sulfate heptahydrate] and allowed to equilibrate *via* vapour diffusion over 1 ml well solution at 298 K. The iron-saturated C-terminal lobe was also crystallized using the same crystallization conditions (Sharma *et al.*, 2003). Irregular-shaped colourless crystals appeared in 2 d and grew to final dimensions of 0.5 × 0.3 × 0.3 mm. These crystals were transferred to 25%(*v*/*v*) polyethylene glycol monomethyl ether 550 in 25 m*M* sodium acetate buffer, the pH of which was gradually lowered from 6.5 to 3.8. At this pH, the crystals were stable.

2.6. Data collection

X-ray intensity data were collected at 283 K on a MAR 345dtb imaging-plate detector using Cu $K\alpha$ radiation from a Rigaku RU-300 rotating-anode generator operating at 100 mA and 50 kV. The data, which extended to approximately 2.0 Å resolution, were processed using *DENZO* (Otwinowski & Minor, 1997) and scaled and merged using *SCALEPACK* (Otwinowski & Minor, 1997). The observed diffraction pattern belonged to space group $P2_1$, with unit-cell parameters $a = 63.2$, $b = 50.5$, $c = 66.1$ Å, $\beta = 107.4°$. The space group and unit-cell parameters of the present crystal were similar to those obtained for the iron-saturated C-terminal lobe. The crystallographic data statistics are summarized in Table 1.

2.7. Structure determination and refinement

The structure was determined by molecular replacement with the program *AMoRe* (Collaborative Computational Project, Number 4, 1994) using the coordinates of bovine monoferric C-terminal lobe (PDB code 1nkx) as a search model. The topmost solution in the rotation function had a correlation coefficient of 61.7%. The next highest value of the correlation coefficient was below 28%. A translational position was found which yielded an *R* factor of 42% and a correlation coefficient of 78.2%. The packing arrangements of molecules in the unit cell for this solution yielded no unfavourable intermolecular contacts. The positional and temperature-factor refinement was carried out using *REFMAC* (Collaborative Computational Project, Number 4, 1994) against all measured reflections to 2.0 Å resolution. The refinement calculation was interleaved with several rounds of model building with *O* (Jones *et al.*, 1991). The refinement statistics are summarized in Table 2. In the chain-tracing process, the starting amino-acid residue was Tyr342. At the C-terminal end electron density was not observed beyond Ser676, indicating the absence of the C-terminal fragment 677–689. However, extra density corresponding to a C-terminal pentapeptide 681–685 was observed. It further showed connectivity between Cys684 of the pentapeptide and

Table 3
Distances in metal- and anion-binding sites in the cleft.

Bonds	Distance (Å)
Metal (Zn1)—ligand bond lengths	
Zn—Asp395 $O^{\delta1}$	2.11
Zn—Tyr433 OH	2.05
Zn—Tyr526 OH	1.98
Zn—His595 $N^{\varepsilon2}$	2.27
Zn—O1 (carbonate)	2.28
Zn—O2 (carbonate)	2.27
Carbonate hydrogen-bond lengths	
O1—Arg463 N^{ε}	2.69
O1—Arg463 NH2	2.70
O2—Ala465 N	2.72
O3—Thr459 $O^{\gamma1}$	2.65
O3—Gly466 N	2.95

Table 4
Coordination bond lengths with Zn^{2+} ion (on the surface).

Metal—ligand bond	Distance (Å)
Zn2	
Zn—Glu659 $O^{\varepsilon1}$	2.40
Zn—Glu659 $O^{\varepsilon2}$	2.26
Zn—Lys386 N^{ζ}	2.34†
Zn—Glu388 $O^{\varepsilon1}$	2.16†
Zn—Glu388 $O^{\varepsilon2}$	2.63†
Zn—OW 192	2.07
Zn3	
Zn—Glu444 $O^{\varepsilon1}$	2.30
Zn—Glu444 $O^{\varepsilon2}$	2.59
Zn—His588 $N^{\varepsilon2}$	2.16†
Zn—OW 68	2.26
Zn—OW 69	2.05
Zn—OW 74	2.96

† From symmetry-related molecules.

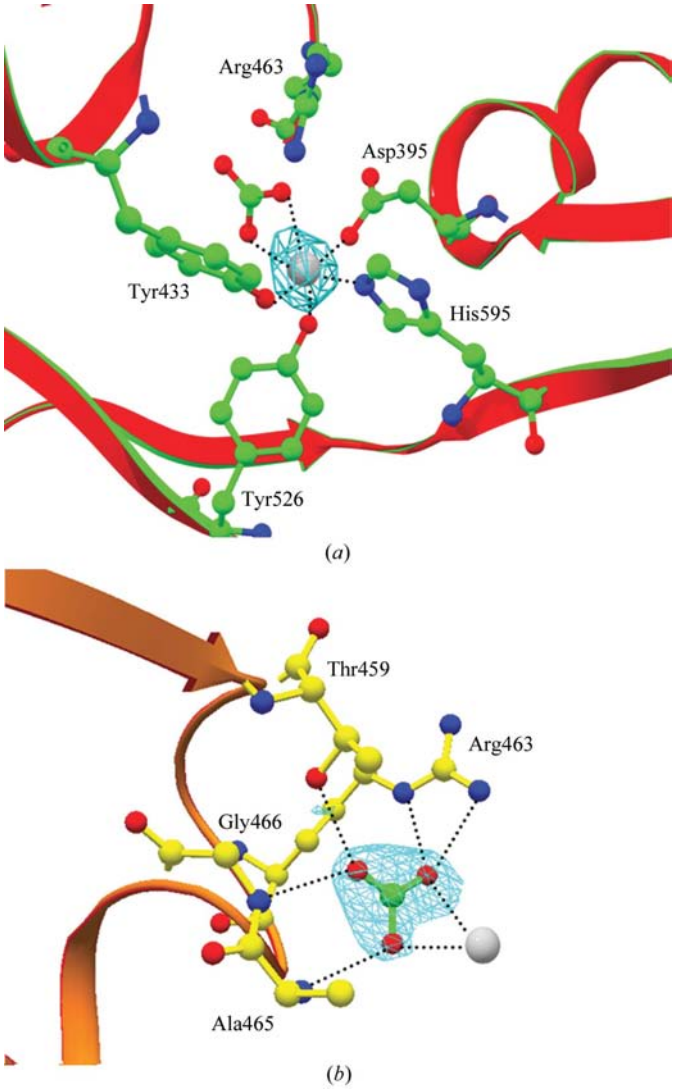

Figure 1
(*a*) The final ($|2F_o - F_c|$) electron density for the zinc ion at the metal-binding cleft drawn at 6σ. The octahedral zinc coordinations are also indicated. (*b*) The final ($|2F_o - F_c|$) electron density for the carbonate anion drawn at 1.5σ. The hydrogen bonds formed involving the carbonate anion are indicated by dotted lines.

Cys405 as in the intact bovine lactoferrin. Electron density for Zn^{2+} (Fig. 1*a*, Table 3) and CO_3^{2-} (Fig. 1*b*, Table 3) and the metal-binding protein ligands was clearly observed. At two additional sites, spherical densities at a 6σ cutoff were also observed (Fig. 2, Table 4). These were interpreted as additional Zn^{2+} ions. The difference electron-density ($|F_o - F_c|$) map also indicated the presence of three carbohydrate chains of different lengths linked to Asn368, Asn476 and Asn545 corresponding to a total of 11 monosaccharide residues (Fig. 3), the largest number of such residues observed so far in any lactoferrin structure. The oligosaccharide chains were refined using bond-length and bond-angle parameters from idealized *N*-acetylglucosamine and mannose units with glycosidic linkages (Jeffrey, 1990). Water molecules were added using the program *ARP* (Collaborative Computational Project, Number 4, 1994). Further rounds of calculation using *REFMAC* interspersed with model building into $|2F_o - F_c|$ and $|F_o - F_c|$ maps led to convergence of the refinement with R and free R factors of 0.192 and 0.210, respectively. The positions of 227 water molecules were determined and included in the model as they met the criteria of having peaks greater than 2.5σ in the $|F_o - F_c|$ map and were hydrogen-bond partners with appropriate distance and angle geometry and had B values of less than 75 Å^2 when refined.

3. Results

3.1. pH-induced zinc/iron-release from C-terminal lobe

Various metal ions have been shown to bind to lactoferrin at the iron-binding site (Smith *et al.*, 1992; Sharma & Singh, 1999; Baker *et al.*, 2000). Similarly, other metal ions are also expected to bind to its isolated C-terminal lobe. It has been reported that zinc-saturated lactoferrin shows higher antibacterial activity compared with its iron-saturated or apo form (Valenti *et al.*, 1987). It has also been shown that all lactoferrins interfere with an early phase of poliovirus infection, but that zinc lactoferrin was the sole form of protein capable of inhibiting a phase of infection subsequent to virus internalization into host cells (Marchetti *et al.*, 1999). The infectious

states generally have acidic pH and the metal-retaining capacity of lactoferrin at acidic pH therefore has important functional significance. The results of a comparative study of the desaturation of the bovine C-terminal lobe for Fe^{3+} and Zn^{2+} ions carried out under identical conditions are shown in Fig. 4. The pH-dependencies of the dissociation of Fe^{3+} and Zn^{2+} ions differ significantly. The onset of iron release begins at pH 5.7, while the corresponding value for Zn^{2+} is 4.6. However, complete desaturation is attained at a similar pH value. Given the fact that the C-terminal lobe retains Zn^{2+} with full occupancy up to a comparatively lower pH value than that for Fe^{3+}, its relevance under certain physiological conditions cannot be ruled out.

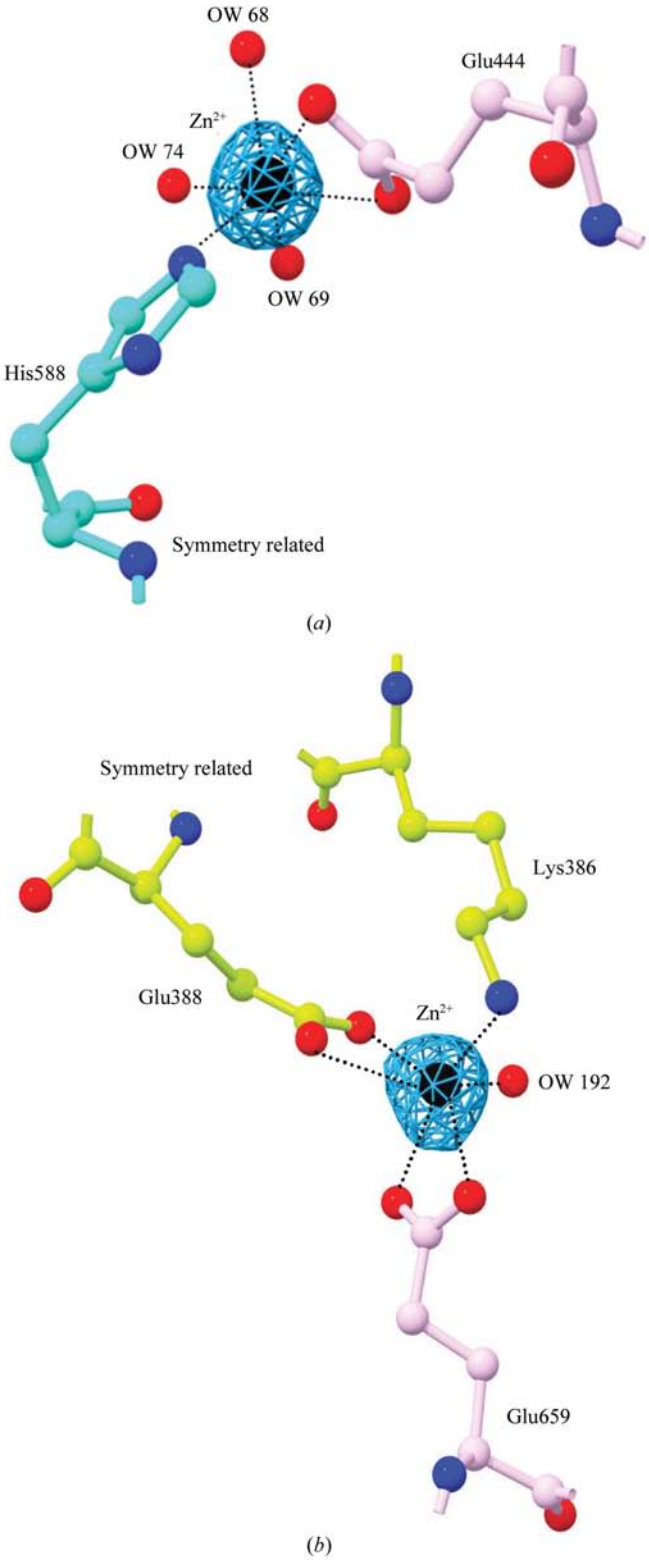

Figure 2
Difference ($|F_o - F_c|$) electron density at 6σ cutoff showing the presence of zinc ion on the surface of the protein. (*a*) Zn^{2+} at site 1 linked to Glu444 and (*b*) at site 2 linked to Glu659. Both zinc ions form distorted octahedral coordination polyhedra.

3.2. Molecular size

The results of DLS experiments gave mean hydrodynamic radii (R_H) for the three samples of 6.94 $\pm$ 0.08 nm for intact lactoferrin, 3.83 $\pm$ 0.08 nm for the monoferric C-terminal lobe and 4.21 $\pm$ 0.08 nm for the zinc-saturated C-terminal lobe. The R_H value of 6.94 $\pm$ 0.08 nm corresponds to a molecular weight of 70–80 kDa, while those of 3.83 $\pm$ 0.08 nm and 4.21 $\pm$ 0.08 nm relate to a molecular weight of about 40 kDa. The difference between the latter two values indicates that the molecular size of the zinc-saturated C-terminal lobe is slightly larger than the monoferric C-terminal lobe; this may be related to its relatively higher degree of flexibility compared with the monoferric C-terminal lobe.

3.3. Overall structure

The structure has been refined to 2.0 Å resolution. The structure was well defined and all residues except an external loop between Arg415 and Cys425 fitted well into the electron density (Fig. 5). The loop Arg415–Cys425 is either mobile or disordered and hence the electron density for this loop was poorly defined. Although the value of the overall temperature factor for the C-terminal lobe is of the order of 40 Å^2, the mean *B* value for the Arg415–Cys425 loop is above 70 Å^2. The *B* value for the corresponding loop in the intact bovine lactoferrin is above 110 Å^2. The model contains 2593 protein atoms from 341 amino-acid residues (Tyr342–Ser676 and Leu681–Ala685), three Zn^{2+} ions, one CO_3^{2-} ion, one sulfate ion, 11 sugar residues and 227 water molecules. The protein molecule has a geometry close to ideal, with r.m.s. deviations of 0.009 Å and 2.1° from standard values for bond lengths and angles, respectively. A total of 88.7% of the residues were found in the most allowed regions of the Ramachandran plot (Ramachandran & Sasisekharan, 1968) as defined in the program *PROCHECK* (Laskowski, MacArthur *et al.*, 1993; Laskowski, Moss *et al.*, 1993). Only one residue, Leu640, with φ, ψ values of 72, −45° was found in the normally disallowed region, but it was the central residue in the formation of a γ-turn (Baker & Hubbard, 1984) that constitutes one wall of the iron-binding cleft in the C-terminal lobe. This γ-turn is conserved in the C-terminal lobe of proteins of the transferrin family. This structure is unique with three metal ions associated with it, one at the regular metal-binding site and two at additional sites on the surface of the protein as intermolecular links.

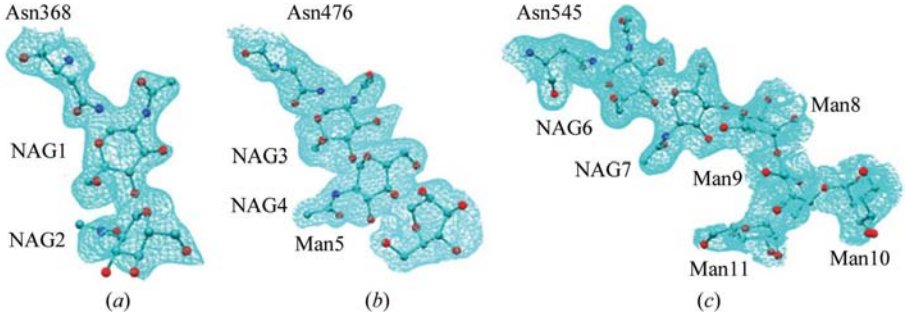

Figure 3
Final electron densities ($|F_o - F_c|$) for the carbohydrate chains at three sites (*a*) Asn368, (*b*) Asn476 and (*c*) Asn545 were contoured at the 1σ level. A total of 11 residues were modelled for three glycan chains at three sites, with two NAG residues at Asn368, two NAG and one MAN residues at Asn476 and two NAG and four MAN residues at Asn545.

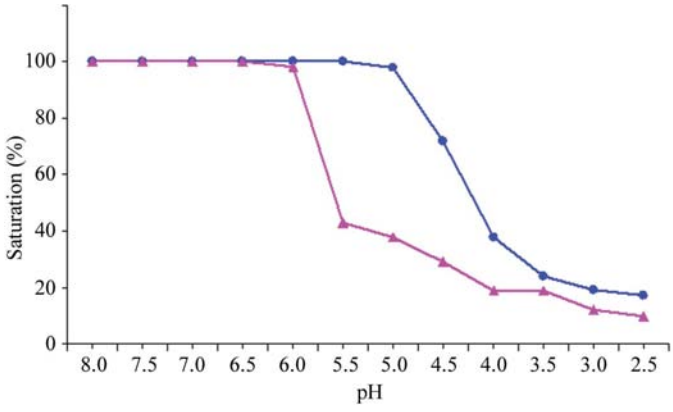

Figure 4
Comparative study of zinc (blue) and iron (magenta) desaturation for bovine C-terminal lobe under identical conditions.

3.4. Molecular structure

The overall molecular structure of the zinc C-terminal lobe is similar to the iron C-terminal lobe (Sharma *et al.*, 2003) with an r.m.s. shift of 0.22 Å in the positions of C^{α} atoms. Proteinase K initially digested lactoferrin at the interlobe region and produced its complete N- and C-terminal lobes. The C-terminal lobe consisted of Tyr342–Ser676 and Leu681–Ala685. In fact, the intact lactoferrin with sequence 1–689 was neatly cut at four places by proteinase K: at Arg341-Tyr342, at Ser676-Thr677, at Leu680-Leu681 and at Ala685-Phe686. These four cleavage sites are structurally located at the interface of the N- and C-terminal lobes. This suggests that the interface is the most susceptible region for enzymatic attack by proteinase K. However, as reported previously (Evan & Williams, 1978; Brines & Brock, 1983; Legrand *et al.*, 1984, 1990), several other proteases have also been used but the desired results were not obtained. It is noteworthy that complete digestion of lactoferrin does not occur because a proteinase K-inactivating decapeptide is present in the C-terminal lobe of lactoferrin (Singh *et al.*, 1998). During the digestion of lactoferrin by proteinase K, as soon as the decapeptide is released it binds to proteinase K at the active site and inhibits further activity. As shown in Fig. 6, the C-terminal lobe is divided into two domains: C-1 (342–431 + 593–676 + 681–685) and C-2 (432–592). Although the interdomain interactions in the present structure are similar to those observed in the monoferric C-terminal lobe of bovine lactoferrin (Sharma *et al.*, 2003), there are notable variations in the lengths of hydrogen bonds. Generally, the interdomain distances in the present structure are longer than those in monoferric C-terminal lobe (Table 5). The orientations of the residues in the body of the molecule are very similar to those observed in the monoferric C-terminal lobe, but the side chains of several residues on the surface are oriented differently. The domains in the present structure are only marginally less closed (by 0.3°) than those in the iron-saturated C-terminal lobe. However, the mean *B* factors of the protein atoms in the present structure are significantly higher ($B \simeq 39.8$ Å^2) than the corresponding values found in the monoferric C-terminal lobe ($B \simeq 29.5$ Å^2). In addition, the overall size of the zinc-saturated C-terminal lobe as indicated by DLS measurements was slightly larger than the monoferric C-terminal lobe. Although these differences may not appear to be striking, they do indicate that the structure of the zinc-saturated C-terminal lobe at acidic pH is less compact when compared with the monoferric C-terminal lobe. It suggests that on lowering the pH the structure of the C-terminal lobe tends to become more flexible. Further reduction of the pH from 3.8 resulted in the disintegration of the crystals. Hence, this is the lowest limit of pH at which zinc remains bound in the cleft with the crystals intact for X-ray intensity data collection.

3.5. Carbohydrate structure

The sequence of bovine lactoferrin contains three sites with an Asn-*X*-Ser/Thr sequence that can be glycosylated. All these sites are part of the C-terminal lobe and in the present structure all of them (Asn368, Asn476 and Asn545) are extensively glycosylated. High-quality electron density in the difference Fourier map ($|F_o - F_c|$) clearly indicated the presence of two *N*-acetylglucosamine (NAG1 and NAG2) residues linked to Asn368 (Fig. 3*a*). The second glycan chain with two *N*-acetylglucosamine residues (NAG3 and NAG4) and one α-1,4-mannose residue (MAN5) was modelled at Asn476 (Fig. 3*b*). The third glycan chain was linked to Asn545 and was modelled by two *N*-acetylglucosamine residues (NAG6 and NAG7) and four α-1,4-mannose residues (MAN8–MAN11) (Fig. 3*c*). The number of sugar residues modelled in the present structure is the highest observed to date in any member of the transferrin family. In this case, there are 11 sugar residues from three glycan chains, while in the monoferric C-terminal lobe and the C-terminal lobe of intact bovine lactoferrin ten sugar residues were modelled in each

Table 5
Interdomain hydrogen-bond distances (Å) in the Zn^{2+}-saturated C-terminal lobe and the Fe^{3+}-saturated C-terminal lobe.

Hydrogen bonds	Zn^{2+}—C-terminal lobe	Fe^{3+}—C-terminal lobe
Asp395 $O^{\varepsilon 2}\cdots$Thr464 $O^{\gamma 1}$	3.31	3.24
Glu353 $O^{\varepsilon 1}\cdots$Ser519 O^{γ}	2.76	2.60
Glu546 $O^{\varepsilon 2}\cdots$Arg415 N^{ε}	3.77	2.87
Glu551 $O^{\varepsilon 2}\cdots$Asn644 $N^{\delta 2}$	3.35	2.93
Asn551 $O^{\delta 1}\cdots$Thr636 $O^{\gamma 1}$	3.48	3.00
Glu353 $O^{\varepsilon 2}\cdots$Lys367 N^{ζ} (along the wall of the cleft)	4.01	2.72

structure. As seen from Fig. 6, the most extensively glycosylated residue, Asn545, is located on one of the walls of the metal-binding cleft. As a result, the glycan chain linked to it is sandwiched between the two domains. Thus, this glycan chain makes several interactions with protein atoms. It may therefore play some role in interfering with the movement of the hinge in the C-terminal lobe of bovine lactoferrin and thereby help in retaining the metal ion at a lower pH than is commonly observed. In contrast, Asn368 is completely exposed on the surface of domain C-1 and the trajectory of the glycan chain extends away from the molecule. The third glycosylation site involving Asn476 is close to the C-terminus. Unlike the other two glycan chains, this chain does not have any interaction with the protein atoms. As observed in the previous structures, the conformations of Asn-NAG-NAG-Man segments are similar in both glycan chains attached to Asn476 and Asn545. This agrees well with the observation that Asn-linked carbohydrate structures are generally conserved (Imberty *et al.*, 1990; Imberty & Perez, 1995; Moore *et al.*, 1997).

3.6. Crystal packing

In the present structure, the solvent content is approximately 51%, which is similar to that found in the C-terminal lobe of bovine lactoferrin. However, this value is slightly lower than generally observed in the crystals of intact lactoferrin (approximately 55%). This could indicate that the dumb-bell shape of the full lactoferrin molecule is not as compatible as that of the spherical C-terminal lobe with tighter packing in the crystals. The number of intermolecular hydrogen bonds in the crystal structure of C-terminal lobe is also significantly larger than that observed in the crystal structure of native bovine lactoferrin. Although the packing of molecules in the present structure is similar to that observed in the structure of the monoferric C-terminal lobe (Sharma *et al.*, 2003), it differs as it contains two Zn^{2+} and one SO_4^{2-} ions that lend additional stability to the zinc-saturated C-terminal lobe (Fig. 7).

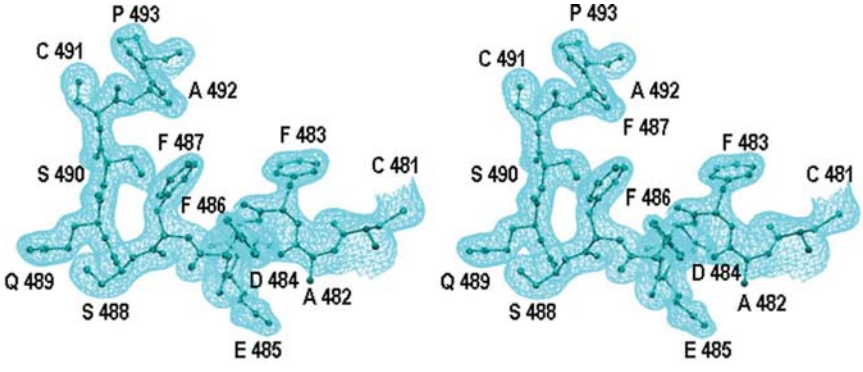

Figure 5
A stereoview of a region of final ($|2F_o - F_c|$) electron-density map contoured at 1.5σ and the corresponding refined model. The diagram was produced using the program *SwissPDBViewer* (Guex & Peitsch, 1997).

4. Discussion

The processes of metal binding and release in lactoferrins are induced by pH and are associated with large-scale conformational changes (Anderson *et al.*, 1989, 1990; Haridas *et al.*, 1995; Moore *et al.*, 1997; Sharma, Paramasivam *et al.*, 1999; Sharma, Kumar *et al.*, 1999; Karthikeyan *et al.*, 1999, 2000; Jameson *et al.*, 1998; Sharma, Rajashankar *et al.*, 1999; Khan *et al.*, 2001; Kumar *et al.*, 2002). A number of structures of metal-saturated lactoferrins at basic pH (Anderson *et al.*, 1989; Haridas *et al.*, 1995; Moore *et al.*, 1997; Sharma, Paramasivam *et al.*, 1999; Sharma, Kumar *et al.*, 1999; Karthikeyan *et al.*, 1999, 2002) and apolactoferrins also at basic pH (Anderson *et al.*, 1990; Jameson *et al.*, 1998; Sharma, Rajashankar *et al.*, 1999; Khan *et al.*, 2001; Kumar *et al.*, 2002) are known. However, no structure of any metal-saturated lactoferrin or a functional domain at acidic pH has yet been reported. It is well known that the metal binding to transferrin and lactoferrin requires a synergistic anion, which is carbonate *in vivo*. The sequestering of metal ions, particularly Zn^{2+} ion, at acidic pH may be of biological significance (Ainscough *et al.*, 1980; Dionysius *et al.*, 1993; Puddu *et al.*, 1998; Marchetti *et al.*, 1999). It was of interest to examine such a structure as it might reveal new features of metal coordination and interdomain relationships. The overall structure of the zinc-saturated C-terminal lobe of bovine lactoferrin even at such a highly acidic pH is essentially similar to the monoferric C-terminal lobe of bovine lactoferrin (Sharma *et al.*, 2003). The r.m.s. shift of the C^{α} atoms when the two structures were superimposed was of the order of 0.22 Å, indicating identical C^{α} tracings. Notable differences were observed in the orientations of some of the important side chains that belong to the interface between the N- and C-terminal lobes in the intact lactoferrin. The relatively weaker hydrogen bonds between the C1 and C2 domains indicate a kind of loosening of the structure. This aspect is also supported by a significantly higher value of an overall temperature factor (39.8 $Å^2$) compared with that of monoferric C-terminal lobe ($B \simeq 29.5$ $Å^2$). The DLS measurements indicated a small increase in the dimensions of the zinc-saturated C-terminal lobe compared with the size of the monoferric C-terminal lobe. These observations, although not large, do indicate that the

lowering of the pH enhances flexibility in the C-terminal lobe. The metal-binding studies indicated that Zn^{2+} remains bound to the cleft in the lactoferrin molecule to a significantly lower pH value (up to 3.8) than that observed for Fe^{3+}, which tends to dissociate at pH 5.0. This is presumably linked to a useful role for the lactoferrin molecule through sequestration of zinc ions under the acidic conditions. It is observed that the presence of Zn^{2+} ions in the Fe^{3+}-binding cleft and on the surface at two specific sites does not alter the structure of the C-terminal lobe. It is noteworthy that all three metal ions have similar sixfold coordinations in the crystal structure. The observed coordination number of six for the zinc ions in the present structure is in agreement with Zn-coordination geometries reported in other structures (Bock *et al.*, 1995; Glusker *et al.*, 1999). The zinc ion in the cleft has slightly shorter coordination distances than those at the intermolecular sites. The C-terminal lobe of bovine lactoferrin is one of the most extensively glycosylated domains in lactoferrins. In the structures of lactoferrins, the values of the *B* factors are found to be generally high (>50 Å^2). Diferric bovine lactoferrin was observed to have one of the highest *B* factors (overall $B \simeq 75$ Å^2), which is much higher than the isolated C-terminal lobe. These values suggest that the individual lobes of lactoferrin can be more tightly packed than the intact protein.

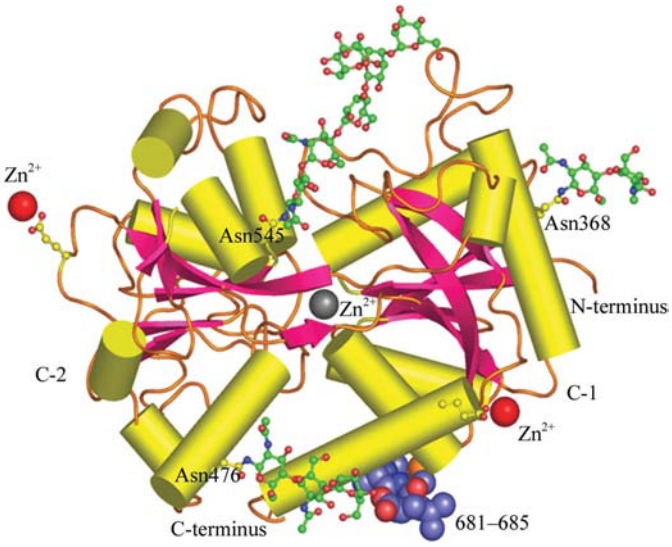

Figure 6
Schematic representation of the C-terminal lobe. Three glycan chains linked to Asn368, Asn476 and Asn545 are shown in ball-and-stick representation. Three zinc ions, one in the metal-binding cleft (grey) and two at the surface (red), are shown. The C1 and C2 domains are also indicated. The hydrolyzed but C–C-linked fragment 681–685 is indicated as a CPK model.

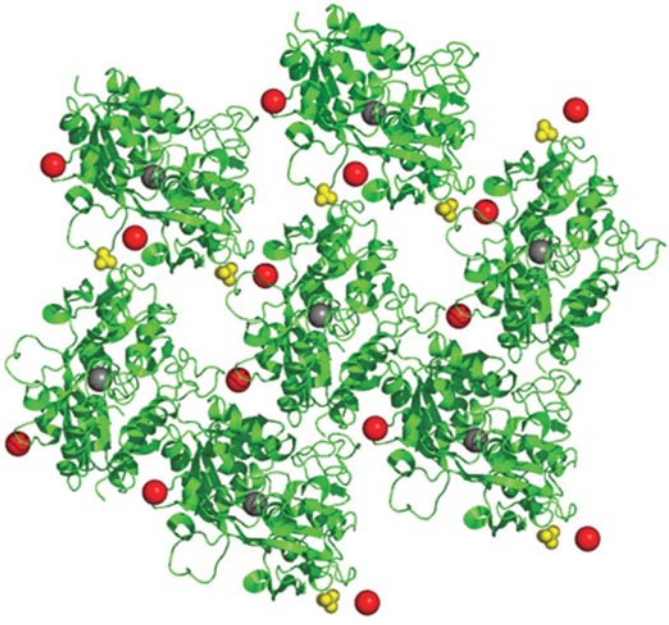

Figure 7
View of the crystal packing showing the locations of zinc ions. The zinc ion in the cleft is shown grey and those at intermolecular site are shown in red. SO_4^{2-} ions are indicated in yellow.

The authors acknowledge financial support from DST, New Delhi under the FIST programme. TJ and NS thank the Council of Scientific and Industrial Research, New Delhi for the award of fellowships.

References

Ainscough, E. W., Brodie, A. M. & Plowman, J. E. (1980). *Am. J. Clin. Nutr.* **33**, 1314–1315.
Anderson, B. F., Baker, H. M., Norris, G. E., Rice, D. W. & Baker, E. N. (1989). *J. Mol. Biol.* **209**, 711–734.
Anderson, B. F., Baker, H. M., Norris, G. E., Rumball, S. V. & Baker, E. N. (1990). *Nature (London)*, **344**, 784–787.
Baker, E. N. & Hubbard, R. E. (1984). *Prog. Biophys. Mol. Biol.* **44**, 97–179.
Baker, H. M., Baker, C. J., Smith, C. A. & Baker, E. N. (2000). *J. Biol. Inorg. Chem.* **5**, 692–698.
Bock, C. W., Katz, A. K. & Glusker, J. P. (1995). *J. Am. Chem. Soc.* **117**, 3754–3765.
Brines, R. D. & Brock, J. H. (1983). *Biochim. Biophys. Acta*, **759**, 229–235.
Brock, J. H. & Arzabe, F. R. (1976). *FEBS Lett.* **69**, 63–66.
Collaborative Computational Project, Number 4 (1994). *Acta Cryst.* D**50**, 760–763.
Day, C. L., Stowell, K. M., Baker, E. N. & Tweedie, J. W. (1992). *J. Biol. Chem.* **267**, 13857–13862.
Dewan, J. C., Mikami, B., Hirose, M. & Sacchettini, J. C. (1993). *Biochemistry*, **32**, 11963–11968.
Dionysius, D. A., Grieve, P. A. & Milne, J. M. (1993). *J. Dairy Sci.* **76**, 2597–2600.
Evan, R. W. & Williams, J. (1978). *Biochem. J.* **173**, 543–552.
Faber, H. R., Baker, C. J., Day, C. L., Tweedie, J. W. & Baker, E. N. (1996). *Biochemistry*, **35**, 14473–14479.
Faber, H. R., Bland, T., Day, C. L., Norris, G. E., Tweedie, J. W. & Baker, E. N. (1996). *J. Mol. Biol.* **256**, 352–363.
Glusker, J. P., Katz, A. K. & Bock, C. W. (1999). *Rigaku J.* **16**, 8–16.
Guex, N. & Peitsch, M. C. (1997). *Electrophoresis*, **18**, 2714–2723.
Haridas, M., Anderson, B. F. & Baker, E. N. (1995). *Acta Cryst.* D**51**, 629–664.
Imberty, A., Gerber, S., Tran, V. & Perez, S. (1990). *Glycoconj. J.* **7**, 27–54.
Imberty, A. & Perez, S. (1995). *Protein Eng.* **8**, 699–709.
Jameson, G. B., Anderson, B. F., Breyer, W. A., Day, C. L., Tweedie, J. W. & Baker, E. N. (2002). *Acta Cryst.* D**58**, 955–962.
Jameson, G. B., Anderson, B. F., Norris, G. E., Thomas, D. H. & Baker, E. N. (1998). *Acta Cryst.* D**54**, 1319–1335.

Jeffrey, G. A. (1990). *Acta Cryst.* B**46**, 89–103.
Jones, T. A., Zou, J. Y., Cowan, S. W. & Kjeldgaard, M. (1991). *Acta Cryst.* A**47**, 110–119.
Karthikeyan, S., Paramasivam, M., Yadav, S., Srinivasan, A. & Singh, T. P. (1999). *Acta Cryst.* D**55**, 1805–1813.
Karthikeyan, S., Yadav, S., Paramasivam, M., Srinivasan, A. & Singh, T. P. (2000). *Acta Cryst.* D**56**, 684–689.
Khan, J. A., Kumar, P., Paramasivam, M., Yadav, R. S., Sahani, M. S., Sharma, S., Srinivasan, A. & Singh, T. P. (2001). *J. Mol. Biol.* **309**, 751–761.
Kumar, P., Khan, J. A., Yadav, S. & Singh, T. P. (2002). *Acta Cryst.* D**58**, 225–232.
Laskowski, R. A., MacArthur, M. W., Moss, D. S. & Thornton, J. M. (1993). *J. Appl. Cryst.* **26**, 283–290.
Laskowski, R. A., Moss, D. S. & Thornton, J. M. (1993). *J. Mol. Biol.* **231**, 1049–1067.
Legrand, G., Mazurier, J., Colavizza, D., Montreuil, J. & Spik, G. (1990). *Biochem. J.* **266**, 575–581.
Legrand, G., Mazurier, J., Metz-Boutigue, M. H., Jolles, P., Montreuil, J. & Spik, G. (1984). *Biochim. Biophys. Acta*, **787**, 90–96.
Lindley, P. F., Bajaj, M., Evans, R. W., Garratt, R. C., Hasnain, S. S., Jhoti, H., Kuser, P., Neu, M., Patel, K., Sarra, R., Strange, R. & Walton, A. (1993). *Acta Cryst.* D**49**, 292–304.
Marchetti, M., Superti, F., Ammendolia, M. G., Rossi, P., Valenti, P. & Seganti, L. (1999). *Med. Microbiol. Immunol. (Berl.)*, **187**, 199–204.
Masson, P. L. & Heremans, J. F. (1968). *Eur. J. Biochem.* **6**, 579–584.
Mizutani, K., Mikami, B. & Hirose, M. (2001). *J. Mol. Biol.* **309**, 937–947.
Mizutani, K., Muralidhara, B. K., Yamashita, H., Tabata, S., Mikami, B. & Hirose, M. (2001). *J. Biol. Chem.* **276**, 35940–35946.
Mizutani, K., Yamashita, H., Kurokawa, H., Mikami, B. & Hirose, M. (1999). *J. Biol. Chem.* **274**, 10190–10194.
Moore, S. A., Anderson, B. F., Groom, C. R., Haridas, M. & Baker, E. N. (1997). *J. Mol. Biol.* **274**, 222–236.
Nicholson, H., Anderson, B. F., Bland, T., Shewry, S. C., Tweedie, J. W. & Baker, E. N. (1997). *Biochemistry*, **36**, 341–346.
Otwinowski, Z. & Minor, W. (1997). *Methods Enzymol.* **176**, 307–326.
Peterson, N. A., Anderson, B. F., Jameson, G. B., Tweedie, J. W. & Baker, E. N. (2000). *Biochemistry*, **39**, 6625–6633.
Peterson, N. A., Arcus, V. L., Anderson, B. F., Tweedie, J. W., Jameson, G. B. & Baker, E. N. (2002). *Biochemistry*, **41**, 14167–14175.
Puddu, P., Borghi, P., Gessani, S., Valenti, P., Belardelli, F. & Seganti, L. (1998). *Int. J. Biochem. Cell Biol.* **30**, 1055–1062.
Ramachandran, G. N. & Sasisekharan, V. (1968). *Adv. Protein Chem.* **23**, 283–438.
Schulze, T. (1996). MSc Thesis. University of Hamburg, Hamburg, Germany.
Sharma, S., Jasti, J., Kumar, J., Mohanty, A. K. & Singh, T. P. (2003). *J. Mol. Biol.* **331**, 485–496.
Sharma, A. K., Kumar, S. & Singh, T. P. (1999). *Indian J. Biochem. Biophys.* **38**, 135–141.
Sharma, A. K., Paramasivam, M., Srinivasan, A., Yadav, M. P. & Singh, T. P. (1999). *J. Mol. Biol.* **289**, 303–317.
Sharma, A. K., Rajashankar, K. R., Yadav, M. P. & Singh, T. P. (1999). *Acta Cryst.* D**55**, 1152–1157.
Sharma, A. K. & Singh, T. P. (1999). *Acta Cryst.* D**55**, 1799–1804.
Sharma, S., Singh, T. P. & Bhatia, K. L. (1999). *J. Dairy Res.* **66**, 81–90.
Singh, T. P., Sharma, S., Karthikeyan, S., Betzel, C. & Bhatia, K. L. (1998). *Proteins Struct. Funct. Genet.* **33**, 30–38.
Smith, C. A., Anderson, B. F., Baker, H. M. & Baker, E. N. (1992). *Biochemistry*, **31**, 4527–4533.
Valenti, P., Visca, P., Antonini, G., Orsi, N. & Antonini, E. (1987). *Med. Microbiol. Immunol.* **176**, 123–130.